VOL. 9, NO. 12, DECEMBER 2014 ISSN 1819-6608
ARPN Journal of Engineering and Applied Sciences


www.arpnjournals.com

DESIGN AND FABRICATION OF A LOW COST PORTABLE SPECTROMETER TO INVESTIGATE OPTICAL PROPERTIES OF THIN FILMS

Benard R. Morumbwa[1], Patrick M. Karimi[1], Daniel M. Wamwangi[2] and Kihara Rurimo[3]
[1]Department of Physics, Kenyatta University, Nairobi, Kenya
[2]School of Physics, University of Witswatersrand, Private Bag, Johannesberg, South Africa
[3]Department of Physics, Jomo Kenyatta University of Agriculture and Technology, Nairobi, Kenya
E-Mail: benardriro@gmail.com

ABSTRACT

Optical spectroscopy is a non-destructive and contactless method for characterizing optical and electrical properties of thin films like reflectance, transmittance, refractive index, permittivity and band gap. These properties determine the application of a thin film as a polarizer, laser, solar cell or photodiode among others. To measure accurately optical properties of thin films, the common types of optical spectrometers used are ellipsometers and spectrophotometers. However these instruments are expensive and there is need to device a cost effective optical spectrometer. In this study, a portable laboratory spectrometer that uses reflectance measurement to determine the optical and electrical properties of thin films was designed. To test the accuracy and reliability of the portable spectrometer designed in this work, reflectance of semiconductor thin film samples of CuO and SnSe were measured using both the designed and a standard spectrometer (SolidSpec-3700). The reflectance measurement for CuO and SnSe had an error of ± 1.88 % and ± 2.17 % respectively, in reference to the standard spectrometer (SolidSpec-3700) reflectance spectra. This error margin is within tolerance level for reliable measurement. In addition the portable spectrometer designed in this work had a resolution of 2 nm ± 5%, cheaper compared to commercially available spectrometers measuring in the same range and portable.

Keywords: spectrometer, diffraction grating, parallel port, reflectance.

1. INTRODUCTION

Several approaches have been adapted for the characterization of the optical properties of thin films. The choice of the approaches taken is determined in part by the nature of excitation studied and on the cost benefit analysis of the method used [1]. In optical characterization two approaches cannot escape unmentioned, namely Raman and Optical spectroscopy which have been widely used as complementary methods. In the study of lattice vibrations, Raman spectroscopy is a suitable choice, whereas optical spectroscopy both in the infra-red (IR), visible (VIS) and deep ultraviolet (UV) provides a dearth of information on the phonon modes, the Plasmon frequencies as well as the band gap of thin films. Among these two approaches their availability in the laboratories is governed by three factors namely cost, simplicity and excitations modes which will be investigated in this study.

Optical spectroscopy within the visible range (380-780 nm) is easy and does not involve complicated equipments like in Raman or Infrared spectroscopy. Most thin films experience high optical absorption in the visible light resulting in a negligible fraction of light being transmitted. Therefore measurements of reflectance are taken in this project [2]. In optical characterization, spectroscopic ellipsometry and optical spectroscopy have found wide spread usage. The former technique relies on the change in the polarization property of light after reflection by a thin film. The concept of measurement for this technique involves the computation of the amplitude ratio upon reflection and the phase difference between the incident and reflected light for determining the optical constants [3]. This approach to optical characterization is complicated and involves expensive sophisticated instruments whose maintenance costs are prohibitive in the long term. However this technique has no match in terms of the speed of measurement and throughput [4].

On the other hand, the commercially available optical spectrometers, which measure reflectance or transmittance, provide a suitable alternative for determining optical properties of thin film. Despite the wide scope of information acquired in optical analysis, this technique is costly and not sustainable for institutions with high financial constraints [5]. Thus there is need to design a simple, fast, cheaper and portable optical spectrometer to determine the optical constants of diverse forms of thin film samples.

The aim of this research is to design and fabricate a low cost portable spectrometer to investigate optical properties of thin films.

2. EXPERIMENTAL SET UP

In this section the hardware and software components of the designed optical spectrometer are discussed. To test the workability of the instrument CuO and SnSe thin film samples were used. Preparation processes of these films are explained, measurement procedure is highlighted and methodology used to determine optical properties of the thin films given.

The designed portable optical spectrometer set up diagram was as shown in Figure-1.

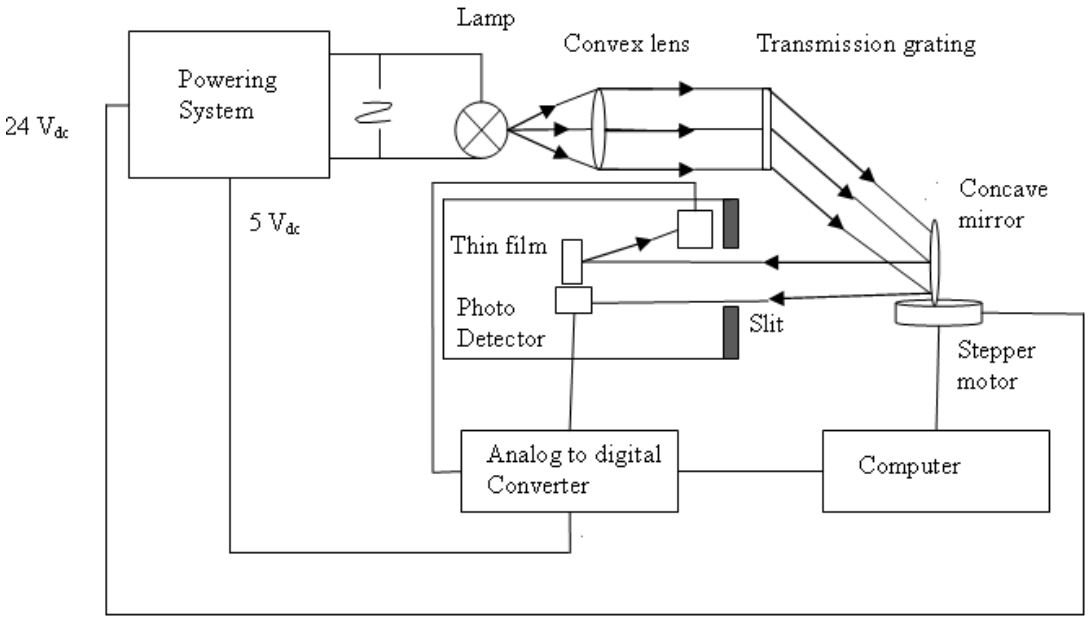

Figure-1. Set up diagram showing hardware components of the portable spectrometer designed in this work.

2.1. Hardware design

The designed portable spectrometer consists of the following components:

a) Powering system;
b) Diffraction system;
c) Stepper motor;
d) Photo-detectors;
e) Analog to digital converter.

2.1.1. Powering system

It consists of the power source (240 Va.c), 240 V to 48 V step down transformer, full wave rectifier, two capacitors, LM317 power regulator and two biasing resistors.

The power indicator and the lamp draw power directly from 240 Va.c. Stepper motor, the clock, analog to digital converter and other electronic components used to automate machine operations require small amount of direct current and voltages. A step down transformer (240V to 48V), full wave rectifier and power regulator are used to rectify alternating current voltage and stabilize it as shown in Figure-2.

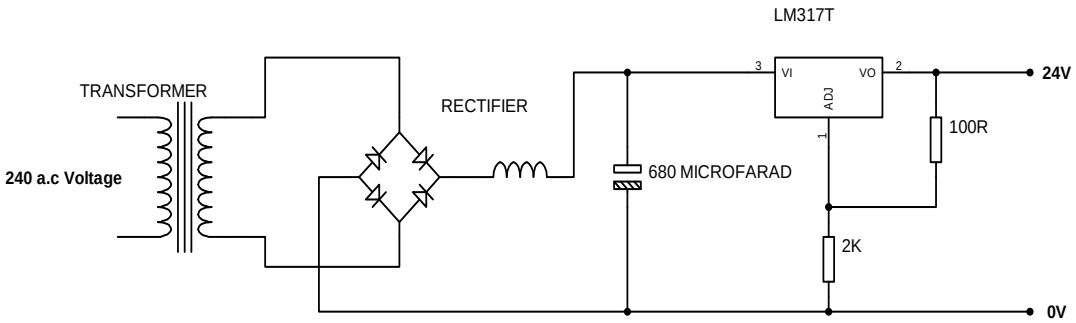

Figure-2. Powering system used to rectify a.c voltage for the portable spectrometer designed in this work.

In the circuit set up the maximum current required is about 1 A and to smoothen the rectified voltage, 680 µF filter capacitor is used, a value obtained by an approximation given by equation 1.

$$c = \frac{IT}{E} \quad (1)$$

Where I = direct current, T = half cycle time, E = a.c voltage component in the rectified voltage, c = capacitance of the smoothening capacitor.

LM317T power regulator is used to stabilize the corrected voltage as to the power requirement of the electronic components in the control circuitry. The power output of the regulator is estimated closely using equation 2.

$$V_o = 1.25V_{DC}\left(1 + \frac{R_2}{R_1}\right) \quad (2)$$

Where V_o = stable output direct current voltage, 1.25 is the converting factor, R_1 = 100Ω resistor, R_2 = determinant resistor which regulates V_o.

2.1.2. Diffraction system

The diffraction system comprises of a fluorescent lamp (250V, 25W) as a source of a wide spectrum (370 - 780 nm). A convex lens (f=5 cm) which produces a parallel beam and focuses it onto the diffraction grating to obtain the visible spectrum. The monochromatic lights obtained are separated from each other at an angular displacement determined by the wavelength of the monochromatic light and the grating constant (1200 lines/mm). This spectrum is then incident onto a concave mirror (f=5 cm) which is controlled by a set of gears (reduction ratio 50:1) driven by a stepper motor, Figure-1. In this work, first order fringes are used because of their high intensity as compared to the higher order fringes. This ensures that the incident and reflected light intensities are easily detectable by the photo-detectors.

2.1.3. Stepper motor

Unipolar stepper motor power rated (500mA, 24V) is used to control small angle rotations of the focusing concave mirror. The ULN2003 driver interfaces the stepper motor to the computer for control. Four control pins (C_0, C_1, C_2, C_3) of an enhanced parallel port are utilized in half stepping the motor, Figure-3. The resolution of the motor used is 7.5° in single stepping mode. Half stepping mode ensures that angle rotations of 3.75° are achieved. Half stepping mode of the rotor involves the mix of single stepping mode and high torque mode. Table-1 summarizes the half stepping mode procedure using the four coils: A1; B1; A2 and B2 of the unipolar stepper motor (PM35S-048).

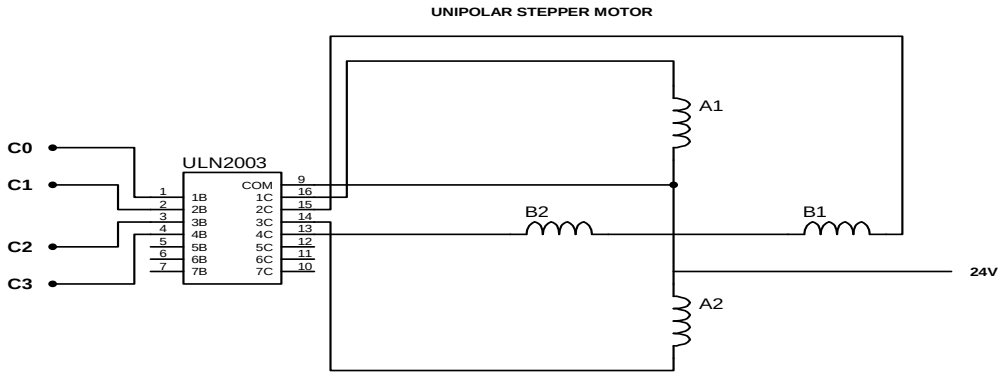

Figure-3. Diagram of circuit used to interface unipolar stepper motor to the enhanced parallel port in the portable spectrometer designed in this work.

Table-1. Unipolar stepper motor half stepping mode procedure.

Pulse	Coil A1 (yellow)	Coil B1 (black)	Coil A2 (orange)	Coil B2 (brown)
1	ON			
2	ON	ON		
3		ON		
4		ON	ON	
5			ON	
6			ON	ON
7				ON
8	ON			ON

2.1.4. Photo-detectors

An aperture allows light to be incident on the first photo - detector and a thin film sample. Specific monochromatic light is focused at a time by a rotation of a concave mirror of focal length 5 cm through small angles (3.75°/50) using a set of gears and a stepper motor. Two silicon photo - detectors are used in this set up as shown in Figure-1. The first one is placed at the same optical path length as the thin film sample from the monochromatic source to record intensity of the incident light. The second is placed 3 cm from the sample along the optical path of the reflected monochromatic beam focused such that it traps the reflected light intensity. The two photo - detectors then convert the light intensities to electrical signals as an input to ADC to produce digital output. From these two readings, incident and reflected monochromatic light intensities, reflectance of the thin film samples is

calculated at various specific radiation wavelengths within the visible range of E.M spectrum.

2.1.5. Analog to digital converter (ADC0809CCN)

The analog to digital converter is powered on by sending a high logic "1" through pin 5 of the parallel port, which switches on the relay switch controlling the converter voltage. Figure-4 shows the pin out diagram for ADC0809CCN.

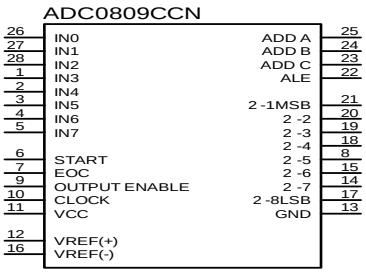

Figure-4. ADC0809CCN Pin out diagram.

The ADC convert the variable analog voltages into digital form to be stored in a computer through the parallel port for analysis. The multiplexer option enables selection of the analog input to be converted by setting address latch enable (ALE) high. In this set up two analog inputs are used hence all the address pins (ADD A, ADD B, ADD C) are tied together and connected to pin 2 (data pin 0) of the parallel port, as illustrated in Figure-5. Selecting incident analog input IN0, a low "0" is sent through pin 2. The reflected monochromatic light (input IN7) is selected by setting pin 2 high "1", as shown in Table-2. Start Conversion (SC) pin is set high and then low to sample analog input and start conversion. According to the manufacturer's specification the ADC requires a delay of 200 µs to convert analog signals to digital form before setting Output Enable (OE) high for reading by the computer port. This procedure is then repeated for all selected analog inputs.

2.2. Software design

2.2.1. Hardware interfacing

The enhanced parallel port was used to interface the portable spectrometer designed in this work with a computer for control and data acquisition. The dialogue between the spectrometer and the computer is initiated using enhanced parallel port (EPP) mode communication protocol (IEEE 1284-A). This allows bidirectional data transfer between the computer and the spectrometer.

2.2.2. MSVC++ 6.0 portable spectrometer driver program designed in this work

The portable spectrometer driver program was developed using Microsoft Foundation Classes (MFC6.0) in VC++ programming environment. VC++ language has extended capabilities in programming and therefore it was chosen in the driver programming. Figure-6 shows a flow chart diagram to summarize the steps which are followed logically during the execution of the portable spectrometer driver program:

Table-2. Input states for the address lines (A, B and C) used to select analog input channel into analog to digital converter (ADC0809CCN).

Selected analog channel	Address line		
	C	B	A
IN0	L	L	L
IN1	L	L	H
IN2	L	H	L
IN3	L	H	H
IN4	H	L	L
IN5	H	L	H
IN6	H	H	L
IN7	H	H	H

The program starts by checking whether the dynamic link library for accessing computer hardware (Enhanced parallel port), Inpout32.dll is installed, if not an error message "Inpout32.dll not loaded" is displayed before it stops. When Inpout32.dll is installed the program checks whether the portable spectrometer designed is connected and it stops if the spectrometer is not connected, displaying "Portable spectrometer is not connected". When the portable spectrometer designed is connected, the program initializes enhanced parallel port registers, measures reflectance, stores data in "optica4.txt" file and displays the data in MS DOS windows before stopping. To measure reflectance, four control pins of the parallel port are utilized to achieve the minimum angle of rotation ($7.5^o \div 2 = 3.75^o$) in a half stepping mode for the stepper motor with step angle resolution of 7.5^o. Half stepping mode involves a mix of single and high torque stepping modes. Eight pulses therefore are required for half stepping mode and then the process is repeated to attain the required angle of rotation. Each pulse gives the stepper motor a rotation of 3.75^o. The binary code generated takes into account the half stepping mode and the fact that all control pins except C_2 are low enable. To rotate the stepper motor through 30^o (8 steps) therefore a decimal code: 10, 14, 15, 13, 9, 1, 3, 2 in this order is written to the control port (890). To reset the rotation a decimal code: 3, 1, 9, 13, 15, 14, 10, 2 is written to the control port as shown in Table-3. The analog to digital converter is controlled by the first three pins of the data port. All the data pins are buffered to enable the computer read data output, ensure unidirectional flow of data from the ADC0809CCN and prevent code mixing in controlling the converter.

Table-3. Binary and decimal code generated by half stepping mode of the unipolar stepper motor.

Pulse	C_3	C_2	C_1	C_0	Decimal
1	1	0	1	0	10
2	1	1	1	0	14
3	1	1	1	1	15
4	1	1	0	1	13
5	1	0	0	1	9
6	0	0	0	1	1
7	0	0	1	1	3
8	0	0	1	0	2

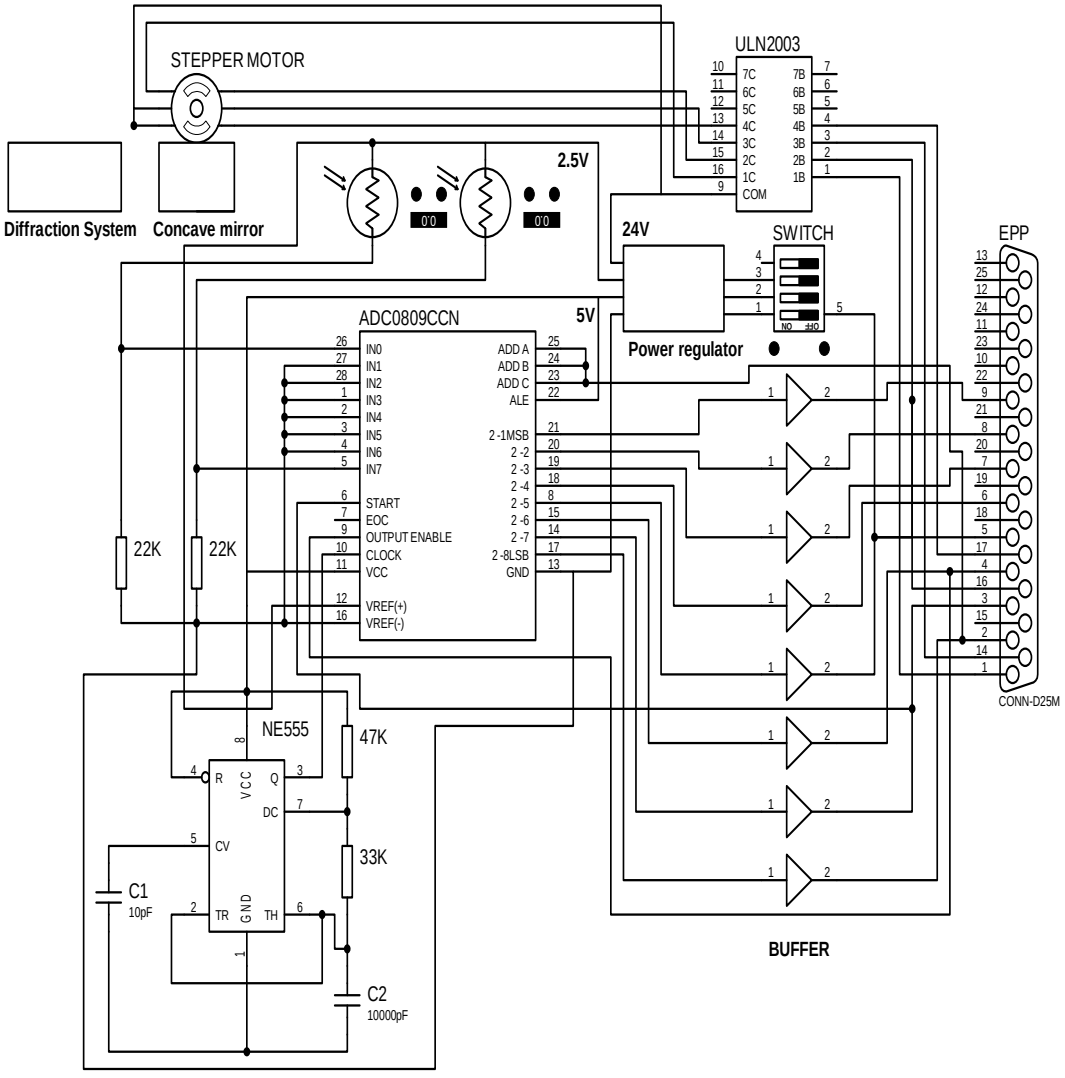

Figure-5. Complete circuit diagram showing the diffraction system, photo-detectors and electronic circuitry of the portable spectrometer designed in this work.

2.3. Preparation of sample thin films

To test the workability of the portable spectrometer designed in this work, thin film samples (CuO and SnSe) were prepared and used to measure the accuracy of the instrument by comparing its results with the standard instrument (SolidSpec-3700).

2.3.1. Preparation of CuO thin film

CuO thin film was prepared by reactive magnetron sputtering using Edward AUTO 306. The silicon glass slide was washed in clean water, rinsed in distilled water and methanol before being dried in the sun for 20 minutes. The glass slide was covered at the ends using aluminium foil to prevent sputtering at the edges. It was then mounted to the substrate holder using clips. Copper target was mounted on the magnetron, maintaining a separation distance of 15 cm between the substrate and the target. The shutter and the chamber were then closed. Argon gas was used as the working gas at the flow rate of 20 sccm, oxygen was used as the reactive gas at a flow rate 5 sccm and other parameters were set as shown by Table-4. Pre- sputtering was done for ten minutes to remove contaminated copper layer. The shutter was then open to allow dislodged copper atoms react with oxygen to form CuO which was then mounted on the substrate.

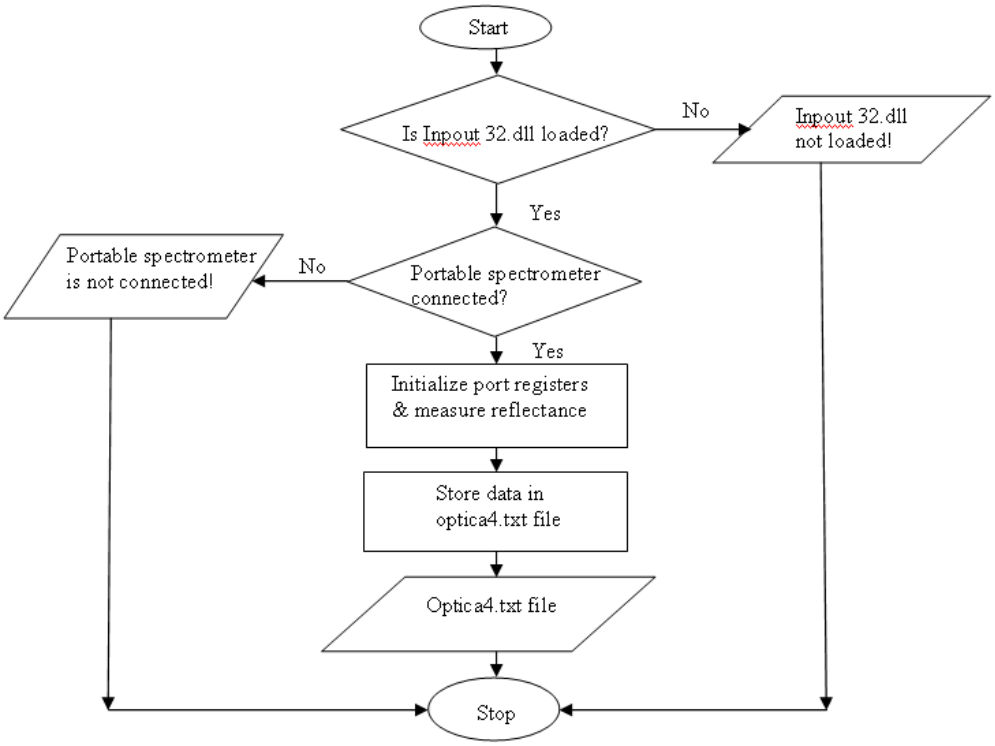

Figure-6. Flow chart diagram for the portable spectrometer driver program.

Table-4. Deposition parameters for CuO thin film used to test portable spectrometer designed in this work.

Thin film	**Argon flow** (sccm)	**Oxygen flow** (sccm)	**Base pressure** (mbars)	**Sputtering pressure** (mbars)	**Power (W)**	**Chamber temperature** (^oC)
CuO	20	5	3×10^{-5}	9×10^{-3}	200	27

2.3.2. Deposition of SnSe

Deposition of tin selenide (SnSe) was carried out using evaporation technique by Edwards AUTO 306. SnSe compound was prepared by mixing tin (Sn) and selenide (Se) in the ratio 1:1 by mass. This mixture was then put into a boiling tube and argon gas blown into the mixture to displace air from the tube while shaking the tube contents during melting process to obtain a homogeneous melt. Deposition chamber was closed and baking was done for ten minutes by heating the boat at a temperature of 500 ^oC to remove air in the evaporation chamber.

Using cleaned glass slide aluminium foiled at the edges as the substrate and the SnSe as the evaporated sample in the molybdenum boat thermal evaporation was carried out. The chamber was closed, pressure reduced to base pressure of 3×10^{-5} mbars, heating current set at 3.5 A and the boat temperature maintained at 750 ^oC, which

was enough to melt the SnSe compound. The deposition parameters are as shown in Table-5.

Table-5. Deposition parameters for SnSe thin film used to test portable spectrometer designed in this work.

Thin film	**Tin** (Sn) **concentration by mass** (%)	**Selenide** (Se) **concentration by mass** (%)	**Deposition temperature** (^oC)	**Base pressure** (mbars)
SnSe	50	50	750	3×10^{-5}

The shutter was then open to allow SnSe vapour to the substrate, which on cooling formed SnSe thin film. Constant rotation of the substrate holder during deposition process ensured uniform composition and thickness of the thin film formed, this process took about 40 minutes. Heating current was then switched off and the chamber opened after an hour to allow cooling which reduced chances of oxidation.

2.4. Measurement procedure of a portable spectrometer designed in this work

The experiment was carried out in a black box to minimize the effects of ambient light as a source of secondary reflections in the visible range. The measurement procedure was performed in three steps as follows:

a) Calibration of the light source: This was a preliminary calibration to measure the intensity of light source. The significance of this calibration was to monitor the fluctuations of incident light due to aging as well as the accurate determination of the optical path. The stepper motor drove a set of gears with reduction ratio 50:1 on which a concave mirror was mounted. The gears further reduced the rotation angle of the motor by a scale of 50; $(3.75^o \div 50) = 0.075^o$. The wavelength of the monochromatic light investigating a sample was selected by the concave mirror rotating the reflected spectrum through constant angle of $(2x0.075^o) = 0.15^o$ in every step the motor rotates. To select the wavelength of electromagnetic radiation within the visible range (370-780 nm) to use in investigating a material, light was passed through a diffraction grating which separated it into monochromatic lights. The angle between monochromatic lights was determined using equation 3 [6].

$$d\sin\theta = n\lambda \quad (3)$$

Where d is the grating constant, n is the order of the fringe, λ is the radiation wavelength and θ is the angle of inclination of a monochromatic light to the principal maxima (fringe). Position of a given monochromatic light in the first order fringe on a screen was given by equation 4.

$$y = D\tan^{-1}\theta \quad (4)$$

Where, D is the separation distance between the diffraction grating and the screen and y the position of the monochromatic light from the central maxima. Using equation 2.3 and 2.4, the resolution wavelength of monochromatic light incident on a sample was determined (2 nm ± 5%). The stepper motor used had an accuracy error of ± 5%. Silver mirror was used to calibrate the source of light since it has a known reflectance profile in the visible range of E.M spectrum. It was also used to check the alignment of optical components to determine whether they were in focus.

b) Measurement: Once the calibration had been done a semiconductor thin film was inserted into the sample stage, the mono-chromatic light was incident at near normal ($\theta < 12^o$) on the first photo-detector and the thin film sample. The intensity of both incident and reflected monochromatic light was then measured using the two photo-detectors and reflectance profile as a function of wavelength obtained.

c) Data acquisition and analysis: The data obtained was transferred and stored in a computer via analog to digital converter through enhanced parallel port (EPP). The portable spectrometer driver program developed in this work was then used to compute reflectance profile and other parameters of CuO and SnSe thin films as follows:

(i) Reflectance, (R)

Reflectance refers to the ratio of incident light intensity which bounces back from a surface. At normal incidence of light to a thin film, reflectance, R is given by equation 5.

$$R = \frac{I_r}{I_o} \quad (5)$$

Where I_r intensity of is reflected light and I_o is the intensity of the incident light. From reflectance measurement of a thin film sample, other optical properties of the sample were obtained as discussed in subsequent sub-sections.

(ii) Real refractive index, (n)

Real refractive index is the ratio of velocity of light in a vacuum to phase velocity of light in a material. It therefore indicates the phase velocity at which light traverses through a material. In normal dispersion, refractive index increases with frequency of incident radiation. At sharp absorptions of radiation energy by a

material, real refractive index deviates from normal dispersion and experiences a reduction which is anomalous dispersion with increase in radiation frequency [7]. Using reflectance measurement, R, in Kramers - Kronig transform [8], the phase angle, ϕ upon reflection of light by a thin film is given by equation 6.

$$\phi(\omega_g) = \frac{4h\omega_g}{\pi} \sum_{j}' \frac{\ln\left[\sqrt{R(\omega_j)}\right]}{\omega_j^2 - \omega_g^2} \quad (6)$$

Where $h = \omega_{j+1} - \omega_j$ and if data interval g is an odd number then $j = 2,4,6,\ldots,g-1,g+1,\ldots$, while if g is an even number then $j = 1,3,5,\ldots,g-1,g+1,\ldots$, and ω_g is the radiation energy at which phase angle is determined. For normally incident light coming from air (real refractive index, $n = 1$ and imaginary refractive index, $k = 0$) into a thin film sample, Fresnel reflectance, R and phase angle, ϕ were used to calculate the real refractive index, n as shown by equation 7.

$$n = \frac{1 - R}{1 + R - 2\sqrt{R}\cos\phi} \quad (7)$$

(iii) Extinction coefficient, (k)

Extinction coefficient, k is also known as the imaginary refractive index. It indicates the extent of radiation energy absorption by a material. Using the reflectance, R and phase change upon reflection ϕ for normally incident light from air to a material, extinction coefficient, k was obtained by equation 8.

$$k = \frac{-2\sqrt{R}\sin\phi}{1 + R - 2\sqrt{R}\cos\phi} \quad (8)$$

(iv) Real dielectric constant, (ε_1)

The electromagnetic field of the incident radiation affects the orientation of positive and negative charges in a thin film. The electric current resulting from this field constitutes conduction and dipole displacement current. Real dielectric constant is also called real permittivity. Real permittivity indicates the radiation energy transmitted through a material medium.

Real permittivity ε_1 is related to real refractive index, n and extinction coefficient, k by equation 9.

$$\varepsilon_1 = n^2 - k^2 \quad (9)$$

(v) Imaginary dielectric constant, (ε_2)

Imaginary dielectric constant is also known as imaginary permittivity, indicates the radiation energy absorbed by a material. The absorbed energy is typically taken up by electrons in the valence band to jump to conduction band and start conducting, constituting electrical energy, scattered or used to heat a material.

Imaginary dielectric constant ε_2 was calculated using real refractive index, n and extinction coefficient, k as indicated by equation 10.

$$\varepsilon_2 = 2nk \quad (10)$$

(vi) Absorption coefficient, (α)

When light traverses through a material, some energy is absorbed. To measure the extent of radiation energy absorption by a material, absorption coefficient, α was determined as shown in equation 11.

$$\alpha = \frac{2\omega k}{c} = \frac{4\pi k}{\lambda} \quad (11)$$

Where c is the speed of light in a vacuum, ω is the cyclic frequency, λ is the radiation wavelength and k is the extinction coefficient.

(vii) Band gap, (E_g)

Semiconductor thin films can be crystalline or amorphous. Crystalline semiconductor thin films have regular arrangement of particles (molecules) in space to create regular shaped crystals. Crystalline semiconductor thin films can be of direct or indirect band gap.

(viii) Direct band gap

A direct band gap occurs when the valence band maximum and the conduction band minimum have the same momentum. The absorption coefficient, α of a semiconductor with a direct band gap obeys equation (2.12) in the region near the band gap [9].

$$\alpha \propto \frac{\sqrt{\hbar\omega - E_g}}{\hbar\omega} \quad (12)$$

Where ħ is reduced Planck's constant = 1.0536 x 10^{-34} Js, E_g is the band gap and ω is the cyclic radiation frequency. Rearranging equation (3.14) we obtain equation (13).

$$(\alpha\hbar\omega)^2 = \hbar\omega - E_g \quad (13)$$

Plotting a graph of photon energy, $\hbar\omega$ against $(\alpha\hbar\omega)^2$ and extrapolating the straight line portion near the edge of the fundamental transition to $(\alpha\hbar\omega)^2 = 0$, the direct band gap was obtained by reading the intercept along the energy axis.

(ix) Indirect band gap

Indirect band gap is experienced when the valence band maximum and conduction band minimum are at different momentum or wave vector. When an electron in the valence band of an indirect band gap semiconductor gains energy above band gap it uses this energy to overcome the band gap and change it is

momentum to reach the conduction band minimum where it can freely conduct.

The absorption coefficient, α of indirect band gap semiconductor is given by equation (14).

$$\alpha \propto \frac{(\hbar\omega - E_g)^n}{\hbar\omega} \quad (14)$$

Rearranging equation (2.14) yields equation (15).

$$\sqrt{\alpha\hbar\omega} = \hbar\omega - E_g \quad (15)$$

Plotting radiation energy, $\hbar\omega$ against $\sqrt{\alpha\hbar\omega}$ and extrapolating the linear portion near the edge of the fundamental transition to $\sqrt{\alpha\hbar\omega} = 0$, the intercept along the energy axis gave the value of indirect band gap.

(x) Band Gap of amorphous semiconductor thin films

In amorphous semiconductor thin films, the band gap is blurred very much because there are many quantum mechanical energy levels outside the actual conduction and valence bands. The absorption coefficient is very small for photon energy below band gap and increases rapidly beyond 10^4 cm^{-1} for radiation energy above the band gap. Therefore the band gap of amorphous semiconductor thin film was defined as the energy at which the absorption coefficient, $\alpha = 10^4$ cm^{-1} [10].

3. Data collection and analysis

To test the workability, reliability and level of accuracy of the portable spectrometer designed in this work, calibration was done using silver mirror, semiconductor thin film samples (CuO and SnSe) were prepared and their optical properties determined using reflectance measurement. Finally comparison on the reflectance measurement and band gap determined using both the portable spectrometer designed in this work and SolidSpec-3700 was done to ascertain the level of accuracy of the designed instrument.

3.1. Instrument calibration

To ensure correct focus of monochromatic light to the thin film sample and the photo-sensors, silver mirror was used because it has a known reflectance profile in the visible spectrum. Silver has good reflectance in the visible spectrum with reflectance above 0.9 and falls significantly in the near ultraviolet range, 380 nm. This was used for initial focus setting of the concave mirror, thus controlling the incidence of monochromatic beam on the film sample and the photo - detectors. Calibration enables the user to detect the variation in intensity of the light source due to aging by observing the changes in the reflectance profile of silver associated with the aging source. The reflectance measurements obtained were compared with silver reflectance graph (standard) from the literature [11] and focus adjustments made until there was a match, an indication that the portable spectrometer designed in this work was now ready for use in measurement. Figure-6 shows a graph of reflectance of silver from literature (Standard), SolidSpec-3700 and the portable spectrometer designed in this work.

The reflectance from SolidSpec-3700 and the portable spectrometer matches well with the standard curve. The difference in reflectance between 450 - 650 nm radiation range was attributed to variation in thickness and surface quality of the silver mirrors which were used.

3.2. Reflectance, (R) of copper oxide (CuO)

Figure-7 shows that the reflectance of CuO reduces with increasing radiation wavelength. The peak at 500 nm can be attributed to inter- band energy transition in CuO. The reflectance measurement by the portable spectrometer designed in this work correlates well with those obtained by SolidSpec-3700. However from 380 - 425 nm it deviates in reflectance measurement from SolidSpec-3700, this may be attributed to reduced sensitivity of the silicon photodiode in the near ultra violet region. The difference in reflectance from 680 - 770 nm is attributed to step position error of the stepper motor used in rotating the concave mirror to focus monochromatic light in the portable spectrometer designed in this work.

3.3. Absorption coefficient, (α) of CuO

Figure-8 shows that the absorption coefficient for CuO increases with decrease of radiation wavelength. The peak at 530 nm is associated with the band gap of CuO. The absorption coefficient values for CuO obtained using SolidSpec-3700 and the portable spectrometer designed in this work compare well with errors noted at the peak value and in radiation wavelengths below 450 nm. These are caused by reduced sensitivity of silicon photodiodes and step position error of the stepper motor.

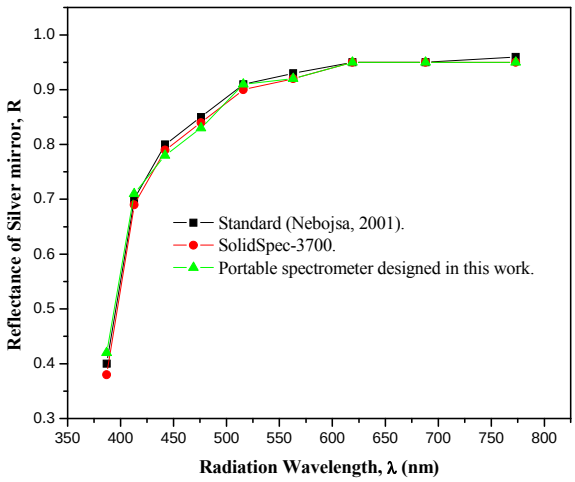

Figure-7. Graph of reflectance against radiation energy for silver mirror using the standard, SolidSpec-3700 and the portable spectrometer designed in this work.

3.4. Band Gap, (E_g) of CuO

Figure-8 shows that a plotted graph of α^2E^2 versus radiation energy, E, was linear from radiation energy 2.2 eV, implying that CuO has a direct band gap. Extrapolating the linear region to where $\alpha^2E^2 = 0$, the x-axis intercept to the line presents the direct band gap of CuO which equals to 2.19 eV ± 1% for both the portable spectrometer designed in this work and SolidSpec-3700 as shown in Figure-8. To draw the linear extrapolation, three points in the linear region were used to minimize error. Accuracy error of the line drawn was estimated using the degree of accuracy used in the horizontal scale of the plotted graph. The horizontal scale used can enable reading up to 0.01 eV and this was the level of accuracy used in determining the band gap.

3.5. Validation of CuO results

There was a maximum error in reflectance of 4.35 % in reflectance measurement of the selected radiation when results of the portable spectrometer designed in this work were compared to those from a standard spectrophotometer (SolidSpec-3700) as shown in Table-6. The mean error was 1.88 % which is within the allowable limits of accuracy for reliable results. The reflectance measurement of CuO by the portable spectrometer designed in this work and SolidSpec-3700 compared well, this is attributed to the high wavelength resolution achieved by small angular rotation of the focusing concave mirror (0.15°). The error in reflectance measurement of CuO was caused by step position error of the stepper motor, low sensitivity of silicon photodiodes used in the region near ultra violet and thermal heating during measurement using the portable spectrometer designed in this work.

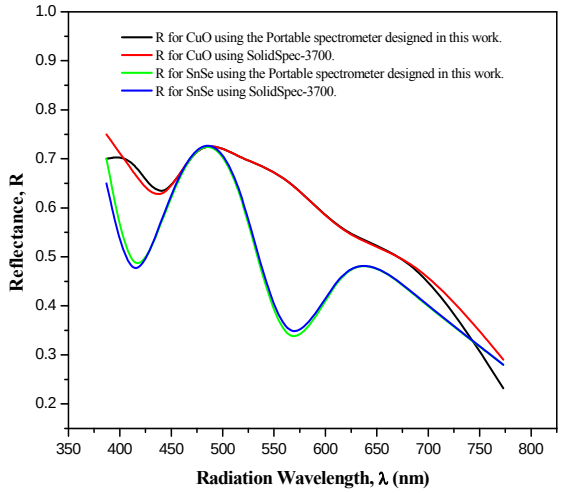

Figure-8. Graph showing reflectance curves for CuO and SnSe thin films from data obtained by SolidSpec-3700 and portable spectrometer designed in this work.

3.6. Reflectance, (R) of tin selenide (SnSe)

Figure-9 shows that SnSe experiences interband energy transition near 650 nm radiation energy in which electrons from the valence band gain enough energy to move into the conduction band to start conducting, thus increasing reflection. The free electrons gain quantum energy to move into high allowable energy levels and emit this energy when they fall back to lower energy levels what causes a reflection peak near 475 nm.

3.7. Absorption coefficient, (α) of SnSe

The absorption of SnSe increased with increase in radiation energy (decrease in wavelength). The absorption of SnSe however is lower than that of CuO as shown in Figure-10.

3.8. Band Gap, (E_g) of SnSe

Figure-11 shows a graph of $\sqrt{\alpha E}$ versus radiation energy for SnSe. The graph is linear near the edge of the fundamental transition implying that SnSe has indirect band gap. To determine the band gap linear extrapolation was done from the linear region to where $\sqrt{\alpha E} = 0$. The x - intercept to the line indicates that the band gap of SnSe equals to 1.22 eV for the portable spectrometer designed in this work and 1.23 eV for SolidSpec-3700 with an accuracy error of ± 1%.

3.9. Validation of SnSe results

The maximum reflectance error for SnSe was 6.38 % when results of the portable spectrometer designed in this work were compared with those obtained by the standard equipment (SolidSpec-3700). The mean error was 2.17 % as shown in Table-6.

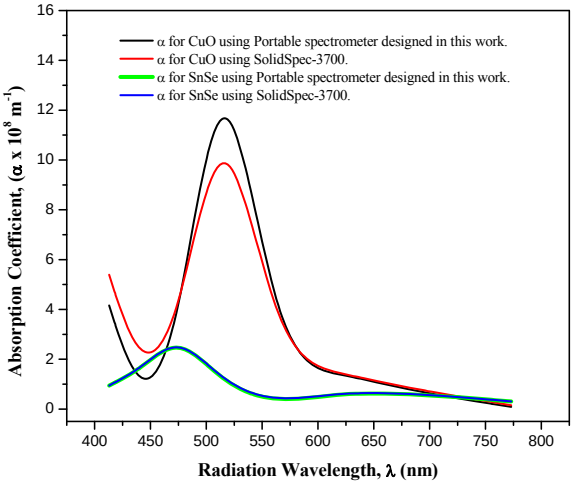

Figure-9. Graph showing the absorption coefficient for CuO and SnSe thin films from data obtained by SolidSpec-3700 and portable spectrometer designed in this work.

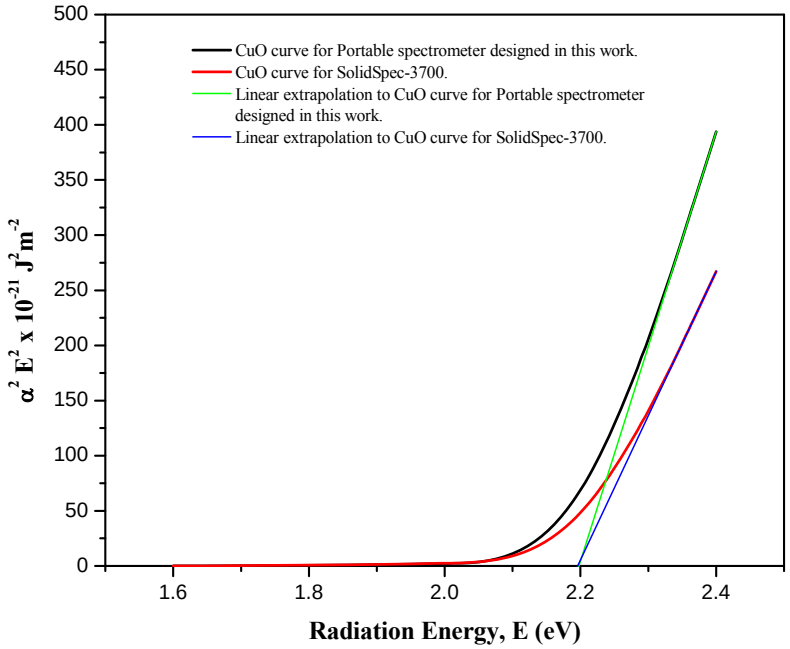

Figure-10. Graph showing linear extrapolation to CuO curves used to determine band gap.

Table-6. Comparison between reflectance of CuO using portable spectrometer designed in this work and spectrophotometer (SolidSpec-3700).

λ (nm)	**Reflectance of CuO using portable spectrometer designed in this work**	**Reflectance of CuO using solidspec-3700**	(%) **Error**
773	0.2200	0.2300	4.35
688	0.5126	0.5118	0.15
619	0.5411	0.5337	1.42
563	0.6697	0.6553	2.17
516	0.7000	0.7000	0.00
476	0.6533	0.6767	3.45
442	0.5279	0.5191	1.69
413	0.7090	0.7000	1.28
387	0.7167	0.7000	2.38
Mean			± 1.88

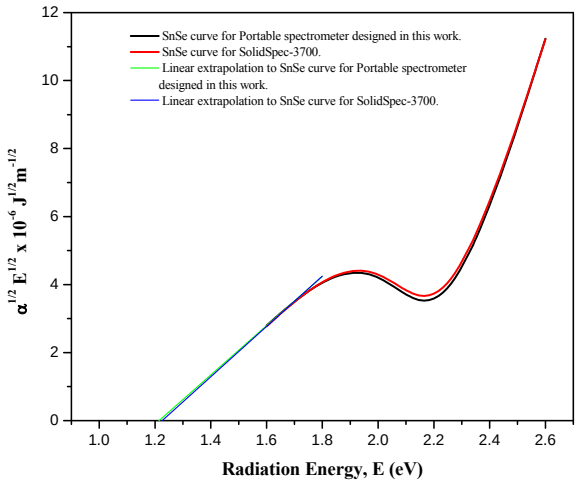

Figure-11. Graph showing linear extrapolation to SnSe curves used to determine band gap.

The mean error was caused by step position error of the stepper motor used in the portable spectrometer designed in this work and the reduced sensitivity of silicon photodiodes to monochromatic light near ultra violet. The measured band gap of SnSe using the portable spectrometer designed in this work compared well with that obtained using standard instrument (SolidSpec-3700) with a marginal error of ± 0.81% as shown in Table-7. The reflectance measurement of CuO and SnSe using the portable spectrometer designed in this work relate well to those of the standard equipment (SolidSpec-3700) with a mean error of ± 2.03 %.

Table-7. Band gap of SnSe using portable spectrometer designed in this work and SolidSpec-3700.

	Film	**Band Gap**
SolidSpec-3700	SnSe	1.23 eV
Designed	SnSe	1.22 eV
Error		0.81%

Table-8. Reflectance of SnSe using the portable spectrometer designed in this work and SolidSpec-3700.

Λ (nm)	**Reflectance of SnSe using portable spectrometer designed in this work**	**Reflectance of SnSe using solidspec-3700**	(%) **Error**
773	0.2317	0.2389	3.01
688	0.5096	0.5159	1.22
619	0.5500	0.5472	0.51
563	0.2130	0.2022	5.35
516	0.7000	0.6941	0.84
476	0.8077	0.7983	1.17
442	0.5879	0.5816	1.07
413	0.3899	0.4165	6.38
387	0.7000	0.7000	0.00
Mean			± 2.17

4. CONCLUSIONS

The designed portable spectrometer in this work measures 38 cm x 30 cm x 14 cm and has a mass of 5 kg. This enables easy movement of the instrument or portability. It consists of a lamp as a source of visible light, a diffraction grating, concave mirror, stepper motor, a set of gears, silicon photo-detectors and analog to digital converter as the main components. These components are common and do not cost much making the portable spectrometer designed in this work total cost to be Kshs. 40 000 which is half the cost of commercially available optical spectrometers measuring in the visible range of the electromagnetic spectrum.

The portable spectrometer uses eight bit analog to digital converter (ADC0809CCN) with a resolution of 9.765625 mV for an analog input range of maximum 2.5 V. This sensitivity ensures that small changes in intensity of monochromatic light are detectable while locking out voltages resulting from background noise (temperature). The set of gears with reduction ratio 50:1 increases angular resolution of the stepper motor to 0.15°. This improves monochromatic light resolution to 2 nm ± 5%. To ensure proper focusing of the monochromatic beam for the correct measurement of reflectance profile of thin film samples, silver mirror was used in calibrating the portable spectrometer designed in this work, increasing reliability and accuracy of the instrument to an average of 97.97 %.

The portable spectrometer designed in this work is recommended to institutions doing research in thin films because of its reliability, accuracy and cost as an alternative to commercially available ones measuring in the same visible range of electromagnetic spectrum.

REFERENCES

[1] Woollam J.A. and Snyder P.G. 1992. Variable Angle Spectroscopic Ellipsometry in: Brundle CR, Evans CA, and Wilson S (eds) Encyclopedia of Materials Characterization: Surfaces, Interfaces, Thin Films, pp. 401-411, Butterworth-Heinemann, Boston, USA.

[2] Frederick W. 1972. Optical Properties of Solids. New York: Academic press. pp. 1-84.

[3] Azzam R.M.A. and Bashara N.M. 1987. Ellipsometry and Polarized Light, Elsevier Science B.V., Amsterdam, Netherlands.

[4] Sidney P. 1993. Optical Characterization of Semiconductors. New York: Academic Press. pp. 1-50.

[5] Pankove I. 1975. Optical processes in Semiconductors. New York: Dover publications. pp. 1-154.

[6] Lipson S. 1996. Optical Physics. 3rd Edn. Cambridge: University press. pp. 106-109.

[7] Carisson K. 2007. Light Microscopy. Error! Hyperlink reference not valid.

[8] Shimadzu. 2008. Spectrophotometric Analysis. No. A228. (Error! Hyperlink reference not valid.).

[9] Kedar Singh, N. S. Saxena, O. N. Srivastava, D. Patidar, T. P. Sharma. 2006. Energy Band Gap of $Se_{100-x}In_x$ Chalogenide Glasses; Banaras Hindu University, Department of Physics, Chalogenide letters. 3(3): 33-36.

[10] Grolik B., Kopp J. 2003. Optical Properties of Thin Semiconductor Films. (http://www.google.com/band gap.pdf).

[11] Nebojsa D. Nikolic et al. 2001. The STM analysis of a silver mirror surface. Journal of Serbian Chemical Society. 66(10): 723-727.